6

Chapter 6

Hydromagnetic Visco-elastic Boundary Layer Slip Flow and Heat Transfer over a Flat Plate

6.1 Introduction

The elastico-viscous fluid has little temperature and salinity sensitivity, and is easily regulated by rheology. The elastico-viscous fluid technology generates highly efficient fractures with low damage to conductivity providing excellent control of fluid loss and high properties of proppant transport to generate geometry of design fractures. The rheology of elastico-viscous fluid are used to enhance biomodeling. Biofilms are also elastico-viscous materials that are capable of dissipating energy from external forces and overcoming external mechanical stresses.

The study of boundary layer flow is very significant in fluid mechanics as the whole dynamics is triggered from the boundary surface. The application of such flow often observed in modern engineering and industrial processes for calculation of frictional drag of bodies. Blasius [45] firstly investigated the structure of evolution of boundary layer fluid velocity over a flat plate. The heat conduction phenomenon of the Blasius problem was

analyzed by Pohlhausen [46]. The numerical computation of Blasius problems carried out by Howarth [47]. Abu-Sitta [103] established the existence of solution for flow past a flat plate. Aziz A [104] presented the solution of thermal boundary layer fluid motion past a flat surface by making use of similarity transformation.

The hydromagnetic fluid motion along with the heat conduction problems over flat plate have been studied extensively these days due to its vast application in industry. Examples includes, petroleum technology, geothermal energy abstractions, aerodynamics, etc. The heat conduction mechanism on a moving metal surface is very significant in production and processing industries like plastic, paper, polymer, etc. The hydromagnetic unsteady heat and mass transport flow problems through porous surface with slip effects studied by Pal and Talukdar [105]. Bhattacharyya *et al.* [106] presented the magnetohydrodynamic Newtonian boundary layer fluid problems past a flat surface with slip effects. Bhattacharyya *et al.* [50] also investigated the boundary layer fluid motion with velocity and thermal slip condition at the boundary over a moving flat sheet.

Velocity slip means non-adherence of the fluid to a solid boundary, is an event that has been often noticed in many circumstances. Recently, many researchers [107-110], studied the fluid motion considering velocity and thermal slip at the boundary as this type of fluid motion has important technological applications. Ambreen et al. [111] discussed the heat transfer mechanism of hydromagnetic non-Newtonian fluid motion with slip effects. Ellahi et al. [112] examined the hydromagnetic boundary layer slip flow past a moving surface with heat conduction and entropy generation.

Inspired by the works mentioned above, the objective of this work is to investigate the steady hydromagnetic visco-elastic boundary layer slip flow and heat transfer characterized by Walters Liquid (Model B') over a flat plate. The partial differential equations governing fluid motion are transformed to ordinary differential equations by making use of suitable similarity variables and solved with the help of bvp4c inbuilt MATLAB software. The computed numerical results are illustrated with graphs and table and discussed for different values of flow parameters involved in the solution.

6.2 Mathematical Formulation

A steady laminar two-dimensional hydromagnetic boundary layer visco-elastic electrically conducting fluid motion with slip effects over a flat plate is considered. The heat transfer

mechanism is also taken into account. The geometrical model of the flow problem is shown in Fig. 6.1. The governing equations of fluid motion and energy are derived taking boundary layer and hydromagnetic approximation as follows:

$$\mathrm{u}\frac{\partial \mathrm{u}}{\partial \mathrm{x}} + \mathrm{v}\frac{\partial \mathrm{u}}{\partial \mathrm{y}} = \nu\frac{\partial^2 \mathrm{u}}{\partial \mathrm{y}^2} - \frac{\mathrm{k}_0}{\rho}\left[\mathrm{u}\frac{\partial^3 \mathrm{u}}{\partial \mathrm{x}\,\partial \mathrm{y}^2} + \mathrm{v}\frac{\partial^3 \mathrm{u}}{\partial \mathrm{y}^3} - \frac{\partial \mathrm{u}}{\partial \mathrm{y}}\frac{\partial^2 \mathrm{u}}{\partial \mathrm{x}\,\partial \mathrm{y}} - \frac{\partial \mathrm{v}}{\partial \mathrm{y}}\frac{\partial^2 \mathrm{u}}{\partial \mathrm{y}^2}\right] - \frac{\sigma B_1^2}{\rho}(U_\infty - u) \qquad (6.2.1)$$

$$\mathrm{u}\frac{\partial \mathrm{T}}{\partial \mathrm{x}} + \mathrm{v}\frac{\partial \mathrm{T}}{\partial \mathrm{y}} = \frac{\mathrm{K}}{\rho C_p}\frac{\partial^2 \mathrm{T}}{\partial \mathrm{y}^2} \qquad (6.2.2)$$

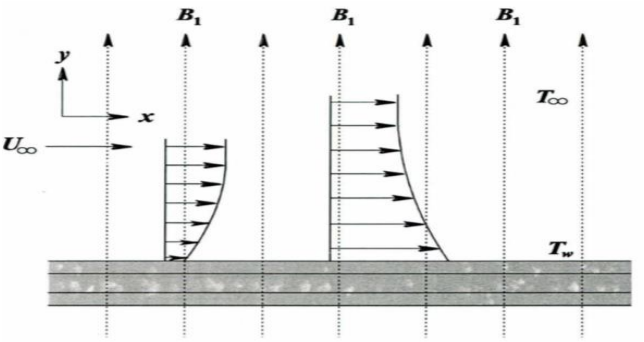

Fig. 6.1 Geometrical model of the flow problem

The relevant boundary conditions for the velocity and temperature taking partial slip into account:

$$u = F_1\left(\frac{\partial \mathrm{u}}{\partial \mathrm{y}}\right), v = 0 \text{ at } \mathrm{y} = 0; \quad u \to U_\infty \text{ as } y \to \infty \qquad (6.2.3)$$

$$T = T_W + G_1\left(\frac{\partial \mathrm{T}}{\partial \mathrm{y}}\right) \text{ at } \mathrm{y} = 0 \;;\; T \to T_\infty \text{ as } y \to \infty \qquad (6.2.4)$$

where $F_1 = F_0(Re_x)^{\frac{1}{2}}$, velocity slip factor with L_0 initial value of slip factor

$G_1 = G_0(Re_x)^{\frac{1}{2}}$, thermal slip factor with D_0 initial value of thermal slip factor

$Re_x = \frac{U_\infty x}{\nu}$, local Reynolds number.

T_W and T_∞ are the assumed constant plate and free stream temperature.

The stream function $\Psi(x, y)$ is introduced as follows:

$$u = \frac{\partial \Psi}{\partial \mathrm{y}} \text{ and } v = -\frac{\partial \Psi}{\partial \mathrm{x}} \qquad (6.2.5)$$

The continuity equation is clearly satisfied automatically by the relation (6.2.5).

Making use of (6.2.5), the equations of momentum (6.2.1) and temperature (6.2.2) transformed as follows:

$$\frac{\partial \Psi}{\partial \mathrm{y}}\frac{\partial^2 \Psi}{\partial \mathrm{x}\,\partial \mathrm{y}} - \frac{\partial \Psi}{\partial \mathrm{x}}\frac{\partial^2 \Psi}{\partial \mathrm{y}^2} = \nu\frac{\partial^3 \Psi}{\partial \mathrm{y}^3} - \frac{\mathrm{k}_0}{\rho}\left[\frac{\partial \Psi}{\partial \mathrm{y}}\frac{\partial^4 \Psi}{\partial \mathrm{x}\,\partial \mathrm{y}^3} - \frac{\partial \Psi}{\partial \mathrm{x}}\frac{\partial^4 \Psi}{\partial \mathrm{y}^4} - \frac{\partial^2 \Psi}{\partial \mathrm{y}^2}\frac{\partial^3 \Psi}{\partial \mathrm{x}\,\partial \mathrm{y}^2} + \frac{\partial^2 \Psi}{\partial \mathrm{x}\,\partial \mathrm{y}}\frac{\partial^3 \Psi}{\partial \mathrm{y}^3}\right] + \frac{\sigma B^2}{\rho}(U_\infty - u) \tag{6.2.6}$$

$$\frac{\partial \Psi}{\partial \mathrm{y}}\frac{\partial \mathrm{T}}{\partial \mathrm{x}} - \frac{\partial \Psi}{\partial \mathrm{x}}\frac{\partial \mathrm{T}}{\partial \mathrm{y}} = \frac{\mathrm{K}}{\rho C_p}\frac{\partial^2 \mathrm{T}}{\partial \mathrm{y}^2} \tag{6.2.7}$$

The transformed boundary conditions of (6.2.3) for the velocity component are

$$\frac{\partial \Psi}{\partial \mathrm{y}} = L_1\frac{\partial^2 \Psi}{\partial \mathrm{y}^2}, \qquad \frac{\partial \Psi}{\partial \mathrm{x}} = 0 \text{ at } \mathrm{y} = 0; \quad \frac{\partial \Psi}{\partial \mathrm{y}} \to U_\infty \text{ as } y \to \infty \tag{6.2.8}$$

Now, introduce the variables Ψ and T in the forms:

$$\Psi = \sqrt{U_\infty \nu \mathrm{x}}\, f(\eta) \text{ and } T = T_w + (T_w - T_\infty)\theta(\eta) \tag{6.2.9}$$

where $\eta = \frac{y}{x}\sqrt{Re_x}$.

Using (6.2.9), the final self-similar equations for governing fluid motion are obtained as follows:

$$f'''(\eta) + \frac{1}{2}f(\eta)f''(\eta) + k_1\left[2f'(\eta)f'''(\eta) + f(\eta)f'^{\mathrm{v}}(\eta) - \left(f''(\eta)\right)^2\right] + \mathrm{M}\left(1 - f'(\eta)\right) = 0 \tag{6.2.10}$$

$$\theta''(\eta) + \frac{1}{2}Prf(\eta)\theta'(\eta) = 0 \tag{6.2.11}$$

where $k_1 = \frac{\mathrm{k}_0 \mathrm{U}_\infty}{2\rho\nu\mathrm{x}}$ and $M = \frac{\sigma B_0^2}{\rho \mathrm{U}_\infty}$ are the modified visco-elastic and magnetic parameters and

$Pr = \frac{\mu C_p}{K}$ is the Prandtl number.

The boundary conditions (6.2.8) and (6.2.4) finally takes the following forms:

$$f(\eta) = 0,\ f'(\eta) = \delta f''(\eta)\ at\ \eta = 0\,; \qquad f'(\eta) = 1,\ f''(\eta) = 0\ as\ \eta \to \infty \tag{6.2.12}$$

$$\theta(\eta) = 1 + \beta\theta'(\eta) \; at \; \eta = 0 \; ; \; \theta(\eta) = 0 \; as \; \eta \; \to \infty \tag{6.2.13}$$

where $\delta = \frac{F_0 U_0}{\nu}$, velocity slip parameter

$\beta = \frac{G_0 U_\infty}{\nu}$, thermal slip parameter.

Boundary condition $f''(\eta) = 0 \; as \; \eta \; \to \infty$ is considered as the fourth physical boundary condition taking into account the fact that at infinity there is no shear stress.

6.3 Method of Solution

The inbuilt numerical method 'bvp4c' of Matlab is a collocation method used to solve differential equations of the form $\frac{dy}{dx} = \mathrm{g(x, y, q)}, \; \mathrm{x} \in [a, b]$ subject to non-linear boundary conditions $\mathrm{h(y(a), y(b), q)} = 0$, where q is an unknown parameter. This method is an effective solver different from the shooting method and it is based on an algorithm. It can compute inexpensively the approximate value of $y(x)$ for any x in $[a, b]$ taking boundary conditions at every step. In this method, infinity conditions at the boundary are replaced with some finite point which reasonably satisfies the given problem.

The self-similar governing equations (6.2.8) and (6.2.9) are transformed to differential equations of the first order as follows:

$$f = f_1, f' = f_2, \; f'' = f_3, f''' = f_4 \; , \theta = f_5, \theta' = f_6 \tag{6.3.1}$$

From (4.3.1), we can write

$$f_1' = f_2, \; f_2' = f_3, \; f_3' = f_4, \; f_5' = f_6 \tag{6.3.2}$$

In view of equations (6.3.1) and (6.3.2), reduced governing equations (6.2.8) and (6.2.9) and boundary conditions (6.2.10) and (6.2.11) can be written as:

$$f_4' = \frac{1}{f_1}\left[(f_3)^2 - 2f_2 f_4 - \left(\frac{1}{k_1}\right)\left\{f_4 + \frac{1}{2}f_1 f_3 + k^*(1 - f_2)\right\}\right] \tag{6.3.3}$$

$$f_6' = -\frac{1}{2} Pr f_1 f_6 \tag{6.3.4}$$

$$f_1(0) = S, f_2(0) = \delta f_3(0) \; and \; f_2(\infty) = 1, f_3(\infty) = 0 \tag{6.3.5}$$

$$f_5(0) = 1 + \beta f_6(0) \; and \; f_5(\infty) = 0 \tag{6.3.6}$$

The MATLAB inbuilt solver 'bvp4c' is employed to compute the above equations together with different involved flow feature parameters.

6.4 Results and Discussion

The nonlinear coupled governing ordinary differential equations (6.3.3) and (6.3.4) together with boundary conditions (6.3.5) and (6.3.6) are numerically solved by MATLAB bvp4c solver for different values of flow parameters. Some figures for velocity, temperature and temperature gradient profiles are plotted and illustrated from physical point of view. The skin friction coefficient (τ) is also computed and displayed in tabular form for various values of magnetic parameter and discussed.

The influence of visco-elastic (k_1), magnetic (M) and velocity slip (δ) parameters on the velocity profiles are shown in Fig. 6.2 to Fig. 6.4. It is observed from Fig. 6.2 that the velocity profile $f'(\eta)$ decreases for a while but gradually it increases with the increasing values of k_1 and consequently the thickness of the boundary layer decreases. Fig. 6.3 depicts the variation in velocity field $f'(\eta)$ for different values of M and it is noticed that fluid motion onward plate reduces as M increases and thus the thickness of boundary layer increases. Physically it is interpreted as drag-like force called the Lorentz force is produced in the fluid flow due to the presence of transverse magnetic field which in turn reduces the fluid motion. The velocity profile $f'(\eta)$ for different values of δ is shown in Fig. 6.4 and it is observed that with the growth of δ, the fluid motion accelerated. The fluid velocity near the plate has some positive value as slip condition act over the plate and thus the thickness of boundary layer diminishes.

The temperature distributions for different values of involved flow parameters are illustrated in Fig. 6.5 to Fig. 6.8. It is observed from Fig. 6.5 to Fig. 6.7 that temperature of the fluid rises with increasing values of k_1, M and δ and gradually it vanishes at some distance from the plate. The heat transfer increases due to enhanced fluid motion and the slip condition at the plate. The temperature distribution is demonstrated from Fig. 6.8 for different values of Prandtl number (Pr). It is noticed that with the growth of Pr fluid viscosity enhances which in turn diminishes the fluid motion and thus the temperature of the fluid reduces. The result shows that with increasing Prandtl number the thermal boundary layer thickness reduces.

The temperature gradient profiles are illustrated from Fig. 6.9 to Fig. 6.11. From Fig. 6.9 to Fig. 6.10, it is observed that with the growth of visco-elastic and magnetic parameters the temperature gradient profiles are initially increasing but gradually decelerate with increasing distance and finally proceeds towards zero. Fig. 6.11 exhibit the temperature

gradient profile for various values of δ and it is noticed that temperature gradient reduces as δ increases initially but after traversing some distance it increases. The numerical values of skin friction coefficient are shown in Table 1 against δ for different values of M. The skin friction coefficient is found to reduce as δ enhances but rises with the growth of M.

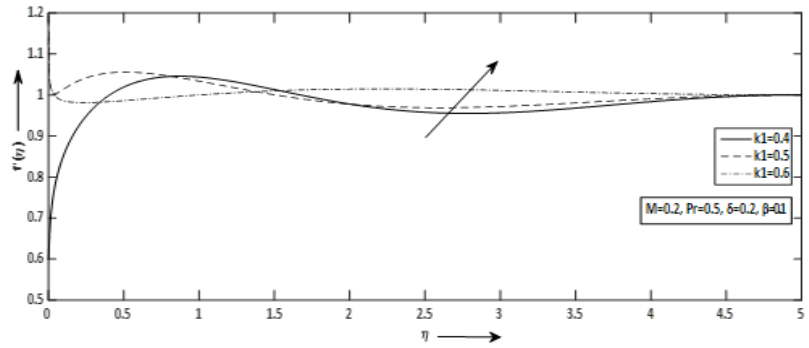

Fig. 6.2 Velocity curves $f'(\eta)$ against η with variation of k_1

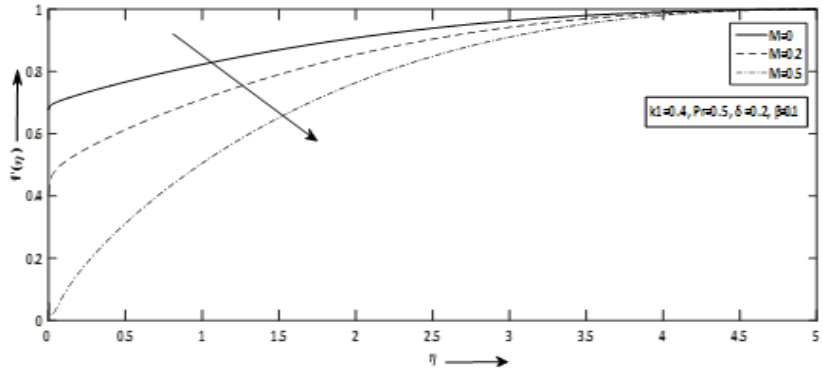

Fig. 6.3 Velocity curves $f'(\eta)$ against η with variation of M

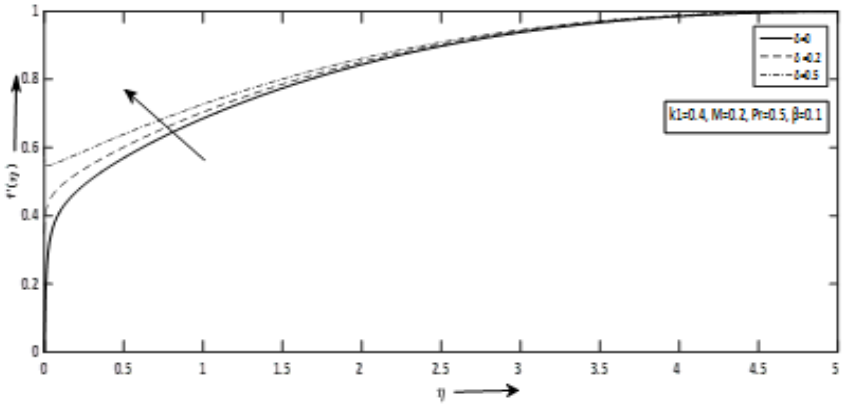

Fig. 6.4 Velocity curves $f'(\eta)$ against η with variation of δ

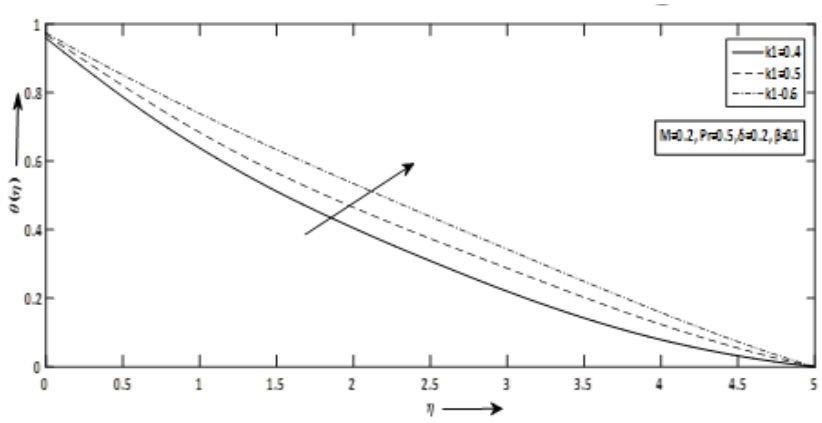

Fig. 6.5 Temperature curves $\theta(\eta)$ against η with variation of k_1

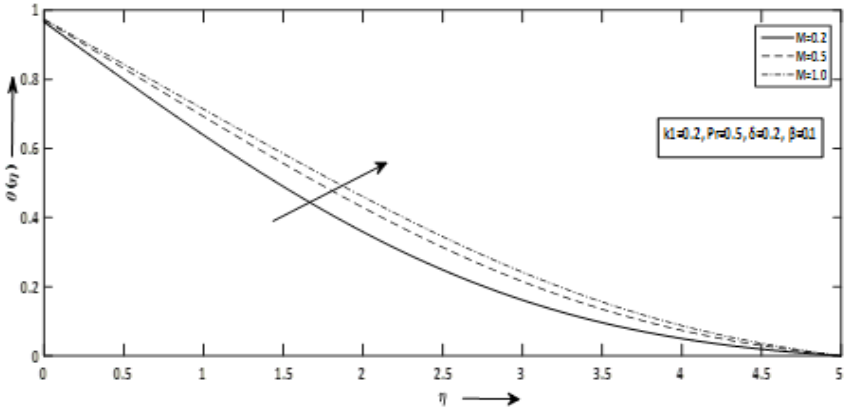

Fig. 6.6 Temperature curves $\theta(\eta)$ against η with variation of M

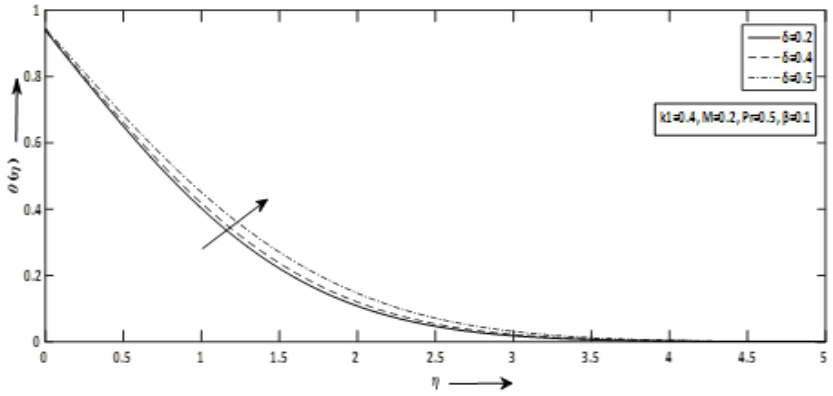

Fig. 6.7 Temperature curves $\theta(\eta)$ against η with variation of δ

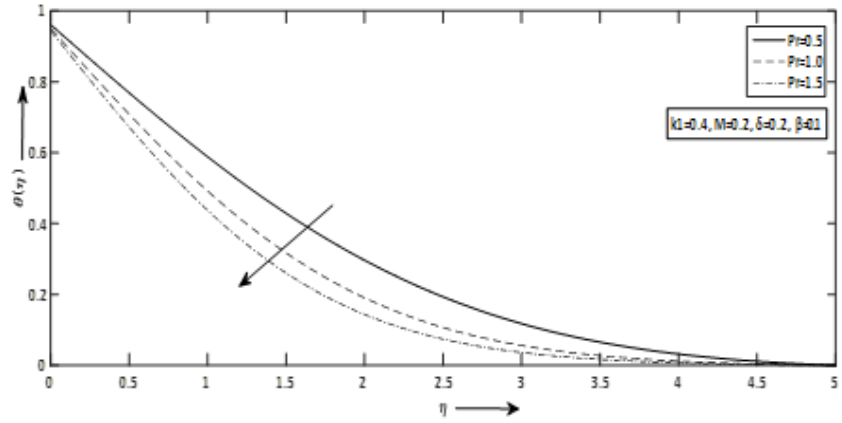

Fig. 6.8 Temperature curves $\theta(\eta)$ against η with variation of Pr

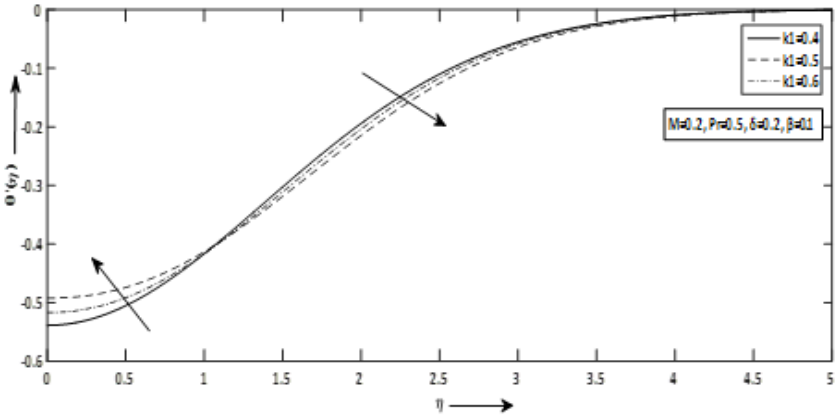

Fig. 6.9 Temperature Gradient curves $\theta(\eta)$ against η with variation of k_1

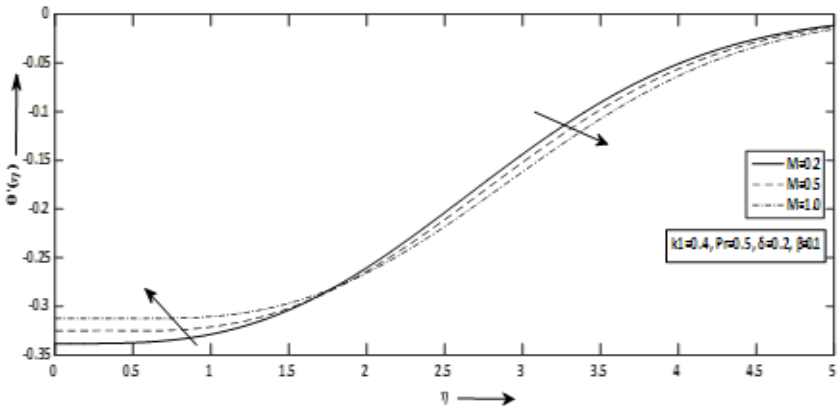

Fig. 6.10 Temperature Gradient curves $\theta(\eta)$ against η with variation of M

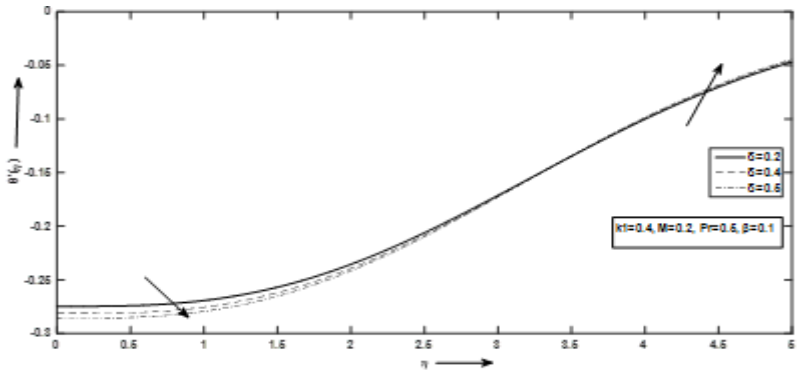

Fig. 6.11 Temperature Gradient curves $\theta(\eta)$ against η with variation of δ

Table 6.1. Numerical values of skin friction coefficient τ for $k_1 = 0.4, Pr = 0.5,\ \beta = 0.1$

Values of skin friction coefficient $\tau = f''(0) + k_1 f(0) f'''(0)$			
Δ	M=0.2	M=0.5	M=1
0	0.6478	0.8231	1.3256
0.2	0.5978	0.6824	1.0467
0.4	0.5246	0.6135	0.8637
0.6	0.4987	0.5831	0.6836
0.8	0.3879	0.4971	0.5783
1	0.2684	0.3257	0.4285

6.5 Conclusion

The study reveals that the hydromagnetic visco-elastic fluid motion is significantly affected by velocity and thermal slip parameters. A future study investigating the flow simulation of the problem would be very interesting. Different numerical and analytical methods can also be implemented to find the solution of the same problem to compare the results.

From the above discussions, the following conclusions can be drawn:

- The rate of transport decreases initially but enhances with the increasing distance (η) and visco-elastic parameter.

- The fluid velocity is found to diminish wth the growth of magnetic parameter.
- The rising values of velocity slip parameter cause to increase the fluid velocity.
- The temperature fluid rises with the growth of visco-elastic, magnetic and slip parameters and gradually it vanishes at some distance from the plate.
- The flow velocity and the temperature diminish with the increase of Prandtl number.The thermal boundary layer thickness decreases with increasing Prandtl number.
- The magnitude of temperature gradient profiles are initially increasing but gradually start decreasing with distance and proceeds towards zero for increasing values of visco-elastic and magnetic parameter.
- The temperature gradient profile initially decreasing but with distance it increases and finally vanishes for increasing values of slip parameter.
- The skin friction coefficient reduces with the increasing values of δ but enhances with the growth of magnetic parameter M.

Scope for Future Work

Viscoelastic fluid flow is an interesting and challenging field of study and offers significant potential for future research and development. It is important to conduct detailed experimental studies to better understand the flow behaviour of viscoelastic fluids. Experiencing ways to control and manipulate the flow of viscoelastic fluids may be practical for many industries, such as polymer processing and improved oil recovery. The development of accurate and efficient numerical models and simulation techniques for the flow of viscoelastic fluids is crucial. Another promising area is the study of viscoelastic fluid behavior in biological and biomedical environments. This includes studying blood flow, mucus flow in the respiratory system, or blood flow in the joints. Research into the application of viscoelastic liquids in various industries such as cosmetics, food processing, oil and gas maybe a fruitful field of research. The development of advanced computational methods and algorithms for solving complex equations governing the flow of viscoelastic fluids is crucial.